sciendo

LATVIAN JOURNAL OF PHYSICS
AND TECHNICAL SCIENCES
2023, N 6

DOI: 10.2478/lpts-2023-0035

SELECTIVE PATTERNED GROWTH OF ZnO NANONEEDLE ARRAYS

I. Mihailova[1,*], M. Krasovska[1], E. Sledevskis[1], V. Gerbreders[1], V. Mizers[1], A. Bulanovs[1], A. Ogurcovs[1,2]

[1] G. Liberts' Innovative Microscopy Centre, Department of Technology, Institute of Life Sciences and Technology, Daugavpils University, 1a Parades Str., Daugavpils, LV-5401, LATVIA
[2] Institute of Solid State Physics, University of Latvia, 8 Kengaraga Str. 8, Riga, LV-1063, LATVIA
*e-mail: irena.mihailova@du.lv

Nanostructured coatings are widely used to improve the sensitivity of various types of sensors by increasing the active surface area compared to smooth films. However, for certain applications (in some cases), it may be necessary to achieve selectivity in the coating process to ensure that nanostructures only form in specific areas leaving interelectrode spaces free of nanostructures. This article discusses several methods for creating intricate ZnO nanostructured patterns, including area selective application of Zn acetate seeds followed by hydrothermal growth, selective thermal decomposition of zinc acetate via laser irradiation followed by hydrothermal growth, and the electrochemical deposition method. These methods enable ZnO nanostructures to grow onto designated surface areas with customised, patterned shapes, and they are rapid, cost-effective, and environmentally benign.

The article examines the process of producing a nanostructured coating with a complex shape and discusses several factors that can impact the quality of the final product. These include the influence of the thermocapillary flows and the "coffee stain" effect on the deposition of a seed layer of zinc oxide from an ethanol solution of zinc acetate. Additionally, the study found that using a protective screen during the growth of nanostructures can reduce the occurrence of unintended parasitic structures in areas lacking a seed layer. Overall, the article presents various techniques and strategies to improve the quality of nanostructured coatings.

We have proven that the use of laser radiation to create a seed layer does not impact the final morphology of the resulting nanostructures. However, when combined with computer-controlled technology, this approach allows for the creation of intricate patterns made up of micrometre-sized lines which cannot be achieved by using other methods.

The article also demonstrates an electrochemical technique for obtaining zinc oxide nanostructures that can selectively coat metal electrodes without requiring a seed layer.

Keywords**:** *Hydrothermal synthesis, nanostructures, selective patterning, ZnO.*

1. INTRODUCTION

At present, nanostructured surfaces have a wide range of applications: solar energy [1], electronics [2], medicine [3], [4], etc. They are also widely used in the development of sensors, proving to be a very effective material for the production of gas sensors [5]–[7], biosensors [8]–[11], and chemical sensors [12], [13]. This is mainly due to the fact that surface nanostructuring significantly enhances sensitivity by increasing the active surface area. Furthermore, the development of nanostructured materials allows for the creation of enzyme-free sensors, which operate based on the direct interaction between analytes and nanostructures [14]–[17]. In a number of cases, this makes it possible to refuse additional functionalisation of the surface with complex organic molecules and enzymes without the loss of sensor sensitivity, which significantly reduces the cost of its production and increases the resistance to mechanical and thermal influences that the sensor is subjected to during production and operation.

There is a large number of physical and chemical methods for obtaining nanostructures, including physical dispersion [18], condensation from liquid [19], [20] and gas phases [21], combustion methods [22], plasma-chemical methods [23], synthesis of nanoparticles from solution [24], [25], sol-gel synthesis [26]–[28], and lithographic [29], [30] and probe methods [31].

Numerous nanostructured materials can be produced using the methods outlined above; however, metal oxide nanostructures, and in particular ZnO, have become widespread. Due to the combination of optical, electrical, and piezoelectric properties of ZnO, it is widely used in optoelectronics and electronic device fabrication [32], [33]. ZnO is biocompatible [34] and relatively stable at biological pH values [35], [36]. This allows for its use as biological markers and as a sensor platform for the detection of different kinds of biomolecules [37]. Hydrothermal synthesis is one of the most promising methods for obtaining metal oxide nanoparticles and epitaxial nanostructured coatings [25], [38]. Compared to other methods of obtaining ZnO nanostructures, hydrothermal synthesis offers a lot of advantages [25], [39]. This method of synthesis is environmentally friendly as it does not require the use of toxic raw materials nor does it generate toxic by-products during the process. Additionally, it is a cost-effective and straightforward approach that does not necessitate expensive raw materials or complex equipment, nor does it require special growing conditions like ultrahigh vacuum, ultrahigh or ultralow temperature and pressure. The synthesis occurs in an aqueous solution at temperatures that typically do not exceed 100 ˚C. The use of relatively low temperatures eliminates the limitations on the types of surfaces that can be coated with nanostructures. This method can be applied to coat any chemically inert surface with nanostructures, including those that are susceptible to high temperatures such as soft polymers, fabrics, and even paper. Hydrothermal synthesis surpasses other nanostructure synthesis techniques in terms of the diversity of morphologies that can be obtained. Our previous studies described in the publication [40] show that ZnO can be obtained in at least 10 different morphologies: nanoparticles, nanoneedles, nanorods, nanoplates, nanoflowers, etc. The standard sample preparation scheme includes the following steps:

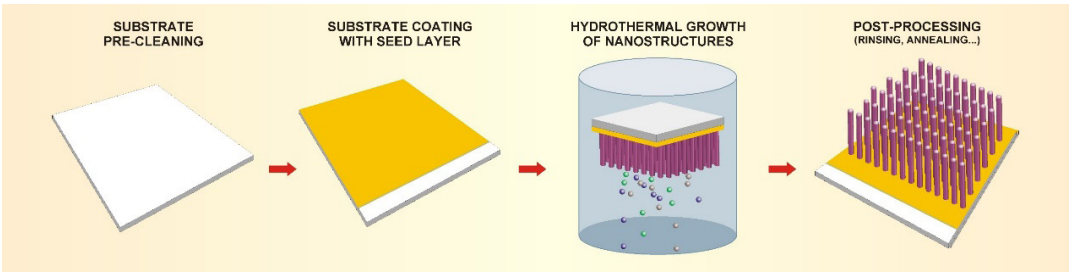

Fig. 1. Basic steps of hydrothermal synthesis.

Sample preparation involves the removal of dirt, grease, and other contaminants from substrate surfaces in order to improve the nanocoating adhesion. A seed layer is used to promote the oriented growth of nanostructures, homogenise the nanostructured coating and improve its adhesion to the surface. The seed layer can be obtained in different ways: magnetron sputtering, electrolytic deposition, etc. However, one of the most popular ways is to use a solution of zinc acetate $Zn(CH_3COOH)_2$ in ethanol which forms a gel-like substance that can be used to coat surfaces of any shape and size and after annealing due to baking to the surface has good adhesion. Equimolar aqueous solutions of zinc nitrate $Zn(NO_3)_2$ and hexamethylenetetramine (HMTA; $C_6H_{12}N_4$) are commonly utilized for the subsequent synthesis of ZnO nanostructures. In this method, $Zn(NO_3)_2$ acts as a source of Zn^{2+} ions, while water functions as a source of O^{2-} ions. HMTA, on the other hand, is a slow-decomposing weak base that produces a slightly alkaline environment in the solution, providing the necessary amount of OH^- ions. When a substrate is immersed in such a solution, the growth of the most prevalent ZnO nanostructure morphology, hexagonal nanorods, occurs.

The following chemical reactions take place during the growth process: [41]

$$C_6H_{12}N_4+6H_2O\rightarrow 6HCHO+4NH_3 \quad (1)$$

$$NH_3+H_2O\rightarrow NH_4^++OH^- \quad (2)$$

$$2OH^-+Zn^{2+}\leftrightarrow Zn(OH)_2 \quad (3)$$

$$Zn(OH)_2\leftrightarrow ZnO+H_2O \quad (4)$$

Other morphologies of ZnO nanostructures can be obtained by changing the composition of the solution and altering the synthesis parameters (growth temperature, time, solution concentration and pH). More details on the influence of various factors on the morphology of nanostructures can be found in our previous articles [42]–[44].

Sometimes the purpose of an experiment requires the surface not to be coated homogeneously over its entire area but rather selectively – maintaining some untreated substrate areas. This issue is especially relevant in the processes of manufacturing various electrodes and sensors.

Selective coatings can be achieved in different ways. First, this can be accomplished by applying the nanostructures only in the specified area using the microprinting method [45]–[48], contact rollers [49], [50], flexographic printing [51], [52] or various types of stamps [53]–[55] and soft moulds (micro-moulds) [56], [57].

In the second case, selective deposition of the seed layer occurs, followed by hydrothermal growth [25], [38], [41]. The publications mention two important factors that greatly affect the quality of selective area

growth that have to be taken into account: the effect of thermal convection in aqueous solutions and the "coffee stain" effect.

Thermal convection can be described as a vertically directed circular motion of a hot fluid that results from differences in density in different parts of the vessel caused by differences in temperature [58], [59]. A large number of ZnO nuclei are generated in the growth solution during the synthesis process. Some of them participate in the formation and growth process of nanostructures, which mostly take place on the pre-coated ZnO seed layer, which is an energetically favourable place. Particles that do not participate in the growth process fall into the precipitate and are drifted into the solution volume by convection flows. When the drifting particles reach the substrate, they can adhere to it and form chaotically oriented second-generation seeds, which cause nanostructure growth in unintended places. To avoid this effect, the sample position in the vessel is very important. The most favourable sample position is in the upper part of the vessel, with the seed-cowered side facing downward. In this case, the minimum contact of the working surface with the nanoparticles drifting in the solution is ensured, and the entire sediment, which cannot be avoided, settles on the non-working surface of the sample. Correspondingly, the most unpropitious position of the sample at the bottom of the vessel since the largest amount of sediment is concentrated there as it settles from the solution under the action of gravity [48]. It should be noted that the correct positioning of the sample reduces the negative effect of the convection flow, but it does not completely eliminate the growth of unwanted nanostructures, so an effective solution to this problem is the use of an additional protective barrier that separates the sample from drifting ZnO nanoparticles and homogenises the solution flow near the sample [47], [60].

The second effect that significantly affects the homogeneity of the nanostructured coating is the "coffee stain" effect [61], [62] and it can be explained as follows. When a drop of the solution reaches the substrate surface, it takes the form of a hemisphere. As there are also solid particles in the drop of solution during the synthesis process, the contact line is fixed, and the temperature in the lower part of the drop is higher than in the upper part. Due to the temperature gradient, the evaporation in some parts of the droplet becomes uneven, which leads to thermocapillary convection and the transfer of particles to the more intense evaporation regions. As a result, particles aggregate on the edge of the former droplet creating a ring-like pattern on the substrate surface [47], [63].

The "coffee stain" effect is observed not only in the case of the selective area growth but also in the case of uniform coating over the entire substrate surface. It occurs when the seeds produced by the acetate route are unevenly distributed over the surface and form annular lines with a high seed density delimiting areas with a low seed density. As a result, it leads to uneven distribution of hydrothermally grown ZnO nanostructures; both cluttered and almost empty areas of irregular shape are observed.

One of the most effective solutions for seed layer surface homogenisation is to use a pre-heated substrate or supply additional heat to the substrate during zinc acetate application. The increased substrate temperature increases the evaporation rate of the solution droplet, which at high values is capable of bypassing the flow of thermocapillary convection directed from the centre to the edge of the drop. Thus, the solution evaporates before the particles begin to collectively migrate towards the edges, allowing them to distribute evenly over the surface.

Another possibility to obtain a selective coating is to use a laser for the selective thermal decomposition of zinc acetate to obtain the seed layer, followed by hydrothermal synthesis of nanostructures. Laser radiation can be used as an effective source of local surface heating, replacing the thermal annealing of a whole sample and thus ensuring area-selective thermal decomposition of zinc acetate and the growth of zinc oxide precursors only in the required place [64], [65]. In some articles, laser irradiation is used not only for producing nanoparticle seeds but also for the nanostructure growth process, completely replacing standard hydrothermal synthesis in the furnace. In this case, the sample surface is irradiated through the working solution layer, and the synthesis of nanostructures takes place only in the heated area. This method ensures a high coating selectivity because in sample areas where the laser beam does not enter, neither the surface nor the solution is heated to the temperature required for hydrothermal synthesis, so the growth of undesirable nanostructures is not possible [66], [67]. The integration of the laser into a computer-controlled scanning system makes it possible to obtain area selective patterns of ZnO seeds and subsequently selective patterning of ZnO nanostructure arrays of any size and shape on the various surfaces.

Sometimes, especially in cases where it is necessary to coat different shapes of metallic electrodes with a nanostructured layer, leaving the space between the electrodes free of nanostructures, it is convenient to apply the electrochemical deposition method. The electrochemical deposition process combines hydrothermal synthesis at a low temperature (<90 °C) and an electrochemical process. The main difference of this method from hydrothermal synthesis is that nanostructures grow only on conductive surfaces where the electrical potential is applied, thus providing area selective deposition and the possibility of obtaining nanostructured electrodes of any shape with element sizes in the range of a few microns.

In the first stage, the precursors dissolve in water and form an electrolyte that contains zinc cations and various types of anions, the chemical composition of which depends on the chosen precursor. In the next step, the oxygen reduction process leads to the formation of hydroxide OH^- ions on the sample's surface, which further interact with the Zn^{2+} ions in solution and generate zinc hydroxide particles. The process ends with the conversion of zinc hydroxide into zinc oxide at an elevated temperature typical of hydrothermal growth.

Precursors based on zinc chloride [68], [69] and zinc nitrate [70], [71] are mainly used. Nitrate-based precursors have one significant advantage: they serve as a source of anions and cations. Nitrate-based precursor reactions can be written as follows.

$$NO_3^- + H_2O + 2e \rightarrow NO_2^- + 2OH^- \quad (5)$$

$$Zn^{2+} 2OH^- \leftrightarrow Zn(OH)_2 \quad (6)$$

$$Zn(OH)_2 \xrightarrow{\text{temperature}} ZnO + H_2O \quad (7)$$

The size and morphology of the resulting nanostructures can be controlled by different additives. For example, [72], [73] indicate that the addition of an electrolyte containing Cl- ions results in the growth of 2D ZnO nanoplates instead of ZnO nanorods. The effect can be explained by the fact that Cl^- ions are mostly adsorbed on the polar ZnO (0002) surfaces of nanowires, blocking growth in the vertical direction and stimulating radial growth in the $\{10\bar{1}0\}$ plane direction. A similar effect is achieved by adding SO_4^{2-} and CH_3COO^- ions to the electrolyte solution [68].

The addition of nitrate-containing support electrolytes (e.g., $NaNO_3$) helps to increase the concentration of OH^- ions without changing the concentration of Zn^{2+} ions and thus change the aspect ratio of the nanostructures, accelerating the growth process similar to hydrothermal growth at elevated pH.

In this article, several methods that allow obtaining area-selective patterns of a ZnO nanorod array are considered. The process of hydrothermal synthesis of rod-shaped nanostructures, as well as the phenomena that affect the uniformity and selectivity of the resulting coating, are considered in detail. The proposed synthesis methods can be used to obtain nanostructured patterns for various purposes. In particular, they can be relevant for the manufacture of electrodes of various shapes, as well as for applications in sensorics.

2. MATERIALS AND METHODS

2.1. Hydrothermal Growth of Patterned ZnO Nanostructure Arrays Based on Selectively Applied Zn Acetate Seeds

In order to investigate the peculiarities of selective growth of ZnO nanostructures, the following samples were prepared. Glass microscope slides (76 x 26 mm) were coated with a 120 nm thick Cr layer, and a 25 mM zinc acetate ethanol solution was applied dropwise to them using a sharp needle. The samples were then annealed for 30 min at 350 ºC and hydrothermally overgrown with ZnO nanoneedles. The composition of the growth solution was 0.025 M $Zn(NO_3)_2$ and 0.05 M HMTA. The growth process took place in a programmable Linn High Therm oven for 1.5 hours at 90 ºC.

In order to ensure additional cleanliness of the sample surface, the glass substrates and the working solution were heated to 90 ºC in an oven separately. This manipulation prevents the condensation of (growth) particles on a cold surface and their accumulation in non-seeded areas, thus preventing the growth of nanostructures in unintended places.

To study the "coffee stain" effect, two groups of samples were obtained. In the first case, an acetate solution was applied onto a substrate at a room temperature, and in the second case, it was applied to a preheated substrate. Furthermore, hydrothermal growth of nanostructures was performed based on the parameters mentioned above.

To evaluate the effect of the protective screen on the growth process of nanostructures, a series of samples were prepared. Some of them were grown as usual by orienting the seed layer facing down in the solution, and some of the samples were grown by enclosing the substrate from the bottom with another glass in such a way that a gap of 2–3 mm formed between the substrate and the screen glass.

2.2. Use of Laser for Area Selective Thermal Decomposition of Zinc Acetate Followed by Hydrothermal Growth

Area selective thermal decomposition of zinc acetate was performed using a Coherent Verdi V-6 532 nm laser integrated with a computer-controlled device with a

mechanised sample positioning platform, which allows control of the trajectory of the laser beam over the sample surface and provides fully automated sample exposure with an accuracy of ± 0.125 μm.

A standard microscope slide was used as a substrate. On top of the slide, a 160 nm thin Cr layer (an effective laser radiation absorbing layer that causes a local temperature increase in the photothermal process) was deposited by magnetron sputtering. Next, a solution of 5 mM Zn $Zn(CH_3COO)_2*2H_2O$ in ethanol was spin-coated on the Cr layer. After complete evaporation of ethanol in air, the sample was irradiated with a laser according to a given trajectory. Scanning was performed at a speed of 55 mm/min with a laser power of - 60 mW.

After irradiation, the samples were subjected to a hydrothermal ZnO growth process.

Samples were placed in equimolar 0.1M solutions of $Zn(NO_3)_2$ and HMTA for 3 h at 90 ºC. At the end of the growth, the samples were rinsed with distilled water. One of them was removed from the glass after rinsing and air-dried. The other was placed in a glass of distilled water and exposed to ultrasound for 2 min to remove unwanted nanostructures that appeared in unirradiated areas and were less bound to the surface compared to nanostructures obtained on ZnO seedlings.

2.3. Electrodeposition Method

Microscope slides were used as the base for a 120 nm thick Cr layer that was deposited by magnetron sputtering through a metal mask to obtain planar circular-shaped electrodes. The ZnO seed layer was produced from an electrolytically coated Zn layer (0.1 M $Zn(NO_3)_2$, j = 90 μA/cm^2, t = 5 min) with subsequent annealing at 350 ºC for 30 min in air, with the aim of oxidising zinc to zinc oxide.

The obtained sample was fixed in a holder, placed in a container containing a growth solution with a lid and connected to the negative pole of the power source. A glass plate covered with a thin Au layer of the same size was used as the cathode. It was fixed in the same holder at a distance of ≈ 1 cm from the anode. The container was placed in the furnace at temperature T = 80 ºC for 2.5 h. Current density, j = 90 μA/cm^2, and voltage, U = 2 V, were maintained during the growth process.

As a working solution, a 0.005 M $Zn(NO_3)_2$ + 0.1 M $NaNO_3$ aqueous solution was used to obtain ZnO nanoneedles and a 0.05 M $Zn(NO_3)_2$ + 0.1 M KCl aqueous solution to obtain ZnO nanoplates.

After the end of the growth process, samples coated with nanostructures were rinsed with distilled water and placed in a furnace at 90 ˚C for 1 h in order to get rid of the remaining solution.

The surface morphology of the processed samples was investigated using a scanning electron microscope (Tescan-Vega II LMU). The chemical composition of the samples was determined by an INCA x-act energy dispersive spectrometer (Oxford Instruments). To determine the structural and phase composition, the XRD spectra were recorded on a Cu Kα (λ = 1.543Å) diffractometer (Rigaku SmartLab) with parallel beam geometry using an additional Ge(220)×2 monochromator.

3. RESULTS AND DISCUSSION

3.1. Selective Application of Zn Acetate Seeds Followed by Hydrothermal Growth

Figure 2 shows the XRD and EDS results of the obtained nanostructures. The resulting nanostructures are well-ordered perpendicular to the substrate and have a high degree of crystallinity. No crystalline phases other than ZnO were detected. Microanalysis results also confirm that the samples are free of chemical impurities.

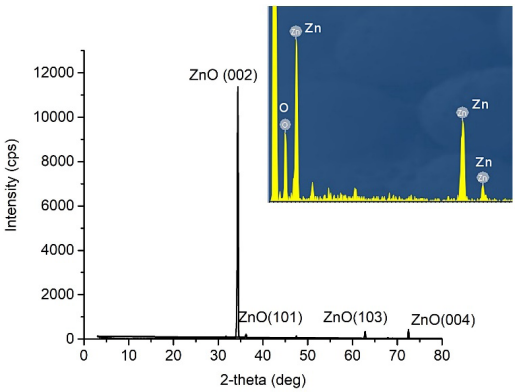

Fig. 2. XRD and EDS microanalysis results of hydrothermally synthesised ZnO nanostructures.

The deviation from the equimolarity of the solution to an excess of HMTA provides an increase in the pH of the solution due to the predominance of OH^- ions and, as a result, an increase in the reaction rate. This allows for reducing the growth time of nanostructures from the standard 3 h [51], to 1.5-2 h. Consequently, reducing the growth time also reduces the probability of unwanted nanostructures appearing.

The results of the analysis of the "coffee stain" effect are summarised in Fig. 3.

Application of zinc acetate solution onto a room temperature substrate leads to the appearance of a ring-shaped formation with a high density of seeds at the edges and sparse, chaotically located seed islets inside the spot. Such a distribution of seeds also determines the growth and distribution of future nanostructures. Figure 3a shows an overview of the droplet after the growth process has ended. As seen in Fig. 3b, the seeding compaction on the edge of the drop contributes to the appearance of densely spaced and vertically aligned ZnO nanoneedles. It should be noted that the width of these bands is relatively small, and when approaching the centre of the drop, the density of the nuclei decreases, and their distribution becomes more uneven. Reduced density of seeds leads to the centre of the droplet being filled with radially arranged 3D ZnO nano-urchins grown on islet formations of seeds (Fig. 3c).

A completely different situation is observed when zinc acetate solution is dropped onto a preheated substrate. Heating the substrate to 100 ºC leads to accelerated evaporation of ethanol compared to the previous case, as evidenced by a fourfold reduction in droplet diameter, thereby reducing the effect of thermocapillary convection. As shown in Fig. 3d, the hydrothermal growth results in a much more homogeneous coating consisting mostly of fine, vertically oriented nanoneedles (Fig. 3e) interrupted in rare areas by densely placed islands of nanoneedles.

The heating of the substrate is also relevant in cases where selectivity is not required, and growth takes place by applying zinc acetate as a continuous layer. In this case, the seed layer becomes more homogeneous, and the distribution of seeds is more even because the areas of compacted seeds, formed as a result of the flow of solution,

disappear. Consequently, the subsequently grown nanostructured coating is also homogeneous.

In Figure 3g, the upper horizontal row illustrates the process of liquid evaporation in a drop in the presence of convection flows. Arrows in the first figure indicate the directions of thermocapillary flows and the presence of areas of thermal inhomogeneities in the droplet. Thus, at the top of the drop, the temperature is lower than at its base, which causes a difference in liquid density and the formation of thermocapillary flows. The middle row illustrates the evaporation process at room temperature for the case when solid particles are present in solution. It can be seen that as the liquid evaporates, the particles are distributed unevenly in solution, forming characteristic dense areas along the edges and rarefied spots in the centre.

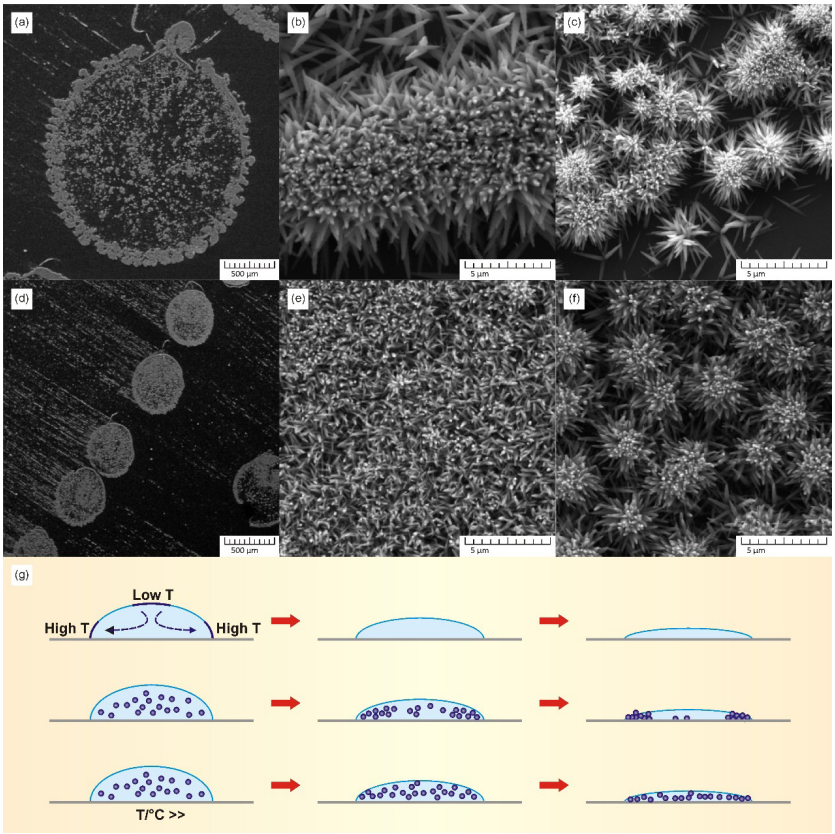

Fig. 3. Analysis of the "coffee stain" effect, where (a), (b), and (c) nanostructures were obtained by applying ZnO precursors on a room-temperature substrate, and (d), (e), and (f) on a pre-heated substrate. Hydrothermal synthesis was carried out in 0.025 M $Zn(NO_3)_2$ and 0.05 M HMTA aqueous solutions at 90 ºC for 1.5 h. (g) Graphic illustration of the coffee stain effect formation process [47].

The bottom row illustrates the evaporation process taking place at an elevated temperature compared to the previous case. In this case, the middle picture shows that the thermocapillary flows do not affect the movement of the particles and they are evenly distributed in the droplet. The results of the experiment using the protective screen are summarised in Fig. 4. As seen in Fig. 4a, if a screen is not used, the

growth of nanostructures occurs both on the seeds layer (droplet) and on the clean glass around the droplet. By placing an additional screen, the growth of nanostructures outside the zinc acetate droplets is suppressed and almost unobservable (Fig. 4b).

Repeating the experiment by changing synthesis parameters (temperature, time, pH of the solution), it was found that in all cases, the result with the application of the screen was many times better than without it.

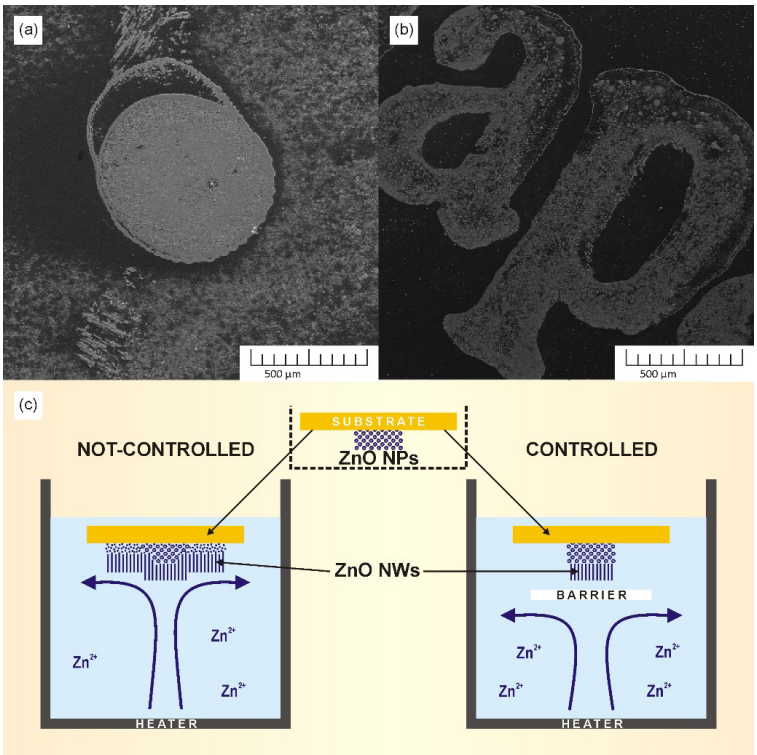

Fig. 4. The effect of the protective screen on the selective coating process, where (a) the growth of nanostructures occurred without and (b) with the protective screen, c) a graphical scheme of the process [60].

This experiment shows that the use of a screen does indeed restrict convection currents and homogenise the solution near the sample while limiting the contact of the sample with the suspension of unwanted sediment particles. This procedure significantly increases the selectivity of the coating and positively affects the quality of the sample.

3.2. Selective Laser Decomposition of Zinc Acetate Followed by Hydrothermal Growth

The stamping method used in the previous chapter to apply zinc acetate to form a nucleation layer is easy to use but has a number of disadvantages. This method is great for creating large patterns, but it is not accurate enough for sharp micron-sized lines. In this case, the laser annealing method proved to be very effective in obtaining a seed layer with a complex shape. Figure 5e shows the process of obtaining nanostructures. Zinc acetate was applied in a continuous layer on a substrate coated with a metal layer to

absorb the temperature. The sample was then irradiated with a laser. Accordingly, the temperature necessary for the thermal conversion of zinc acetate to zinc oxide was reached in places subjected to laser treatment, and a seed layer was formed. The remaining regions of the sample were not subjected to heating; therefore, the zinc acetate in them remained unannealed. Next, the growth of zinc oxide nanostructures occurs according to the standard protocol of hydrothermal synthesis. At the end of the synthesis, the sample is subjected to additional processing in an ultrasonic bath in order to remove parasitic microrods formed in the areas with non-irradiated acetate. As a result, after washing, a nanostructured pattern of a given shape is obtained corresponding to the trajectory of the laser movement.

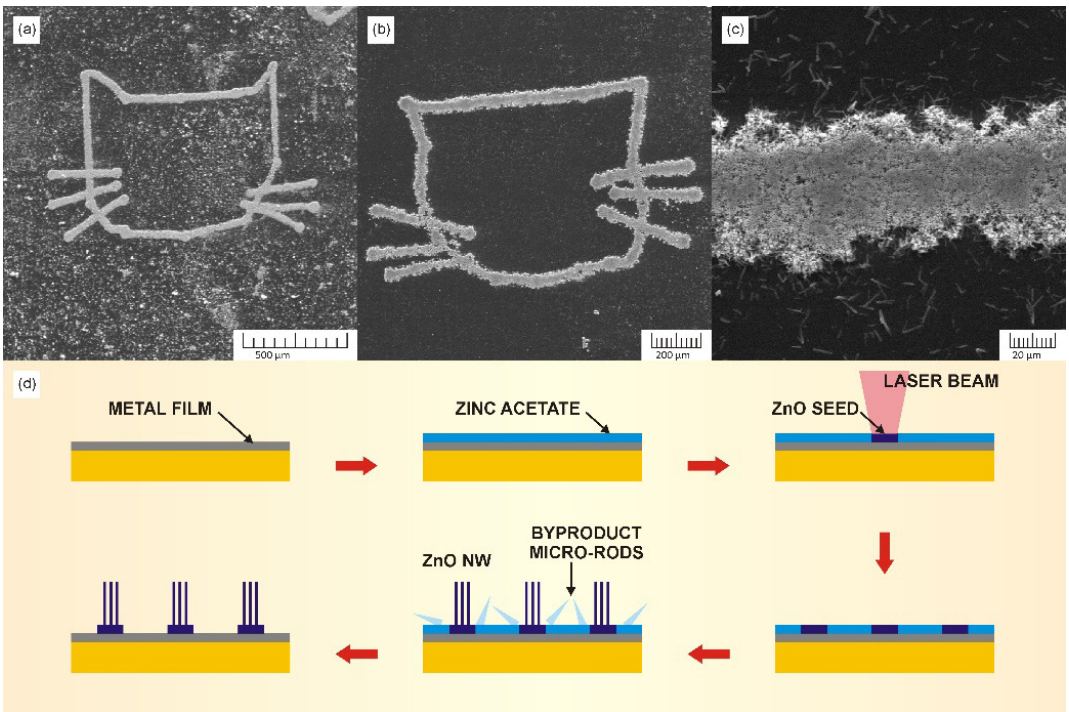

Fig. 5. ZnO nanostructures obtained on areas of selectively laser-assisted seeds with a subsequent hydrothermal growth process in an equimolar working solution (a-c), graphical scheme of the experiment (d) [64].

Most of the articles indicate that even if unwanted by-product microrods appear in places not irradiated with a laser during the nucleation process, their adhesion to the surface is very low since they grow in areas of thermally untreated zinc acetate, and zinc oxide seeds are necessary for the formation of stable adhesion. Such parasitic formations were removed by processing samples in an ultrasonic bath. All nanostructures that do not have sufficient adhesion to the surface are removed, leaving only a clear pattern formed at the site of laser exposure. However, in our case, the situation is different. Practice proves that the efficiency of the method is about 90%. After the ultrasonic bath, the sample's surface becomes significantly cleaner; however, individual unwanted needles can be observed on it. Most likely, the formation of these needles

is related to the good adhesion properties of the Cr thin film. In this case, Cr surface defects become crystallisation centres and induce the formation of nanostructures with adhesion comparable to that provided by the ZnO seed layer.

In order to reduce the number of undesirable nanostructures, a number of articles advise adhering to higher synthesis temperatures or increasing the pH level of the solution when choosing synthesis parameters. This makes it possible to obtain nanostructures of the desired size in a much shorter time, which contributes to a decrease in the density of nanostructures in places without nuclei since such growth is energetically unfavourable.

Our previous studies have shown that the pH level of the working solution and the growth rate of nanostructures can be increased by using a non-equimolar solution (by decreasing the amount of zinc nitrate and increasing the amount of HMTA).

Figure 6 shows the SEM results of a sample obtained in a non-equimolar working solution after subsequent rinsing in an ultrasonic bath after the growth process.

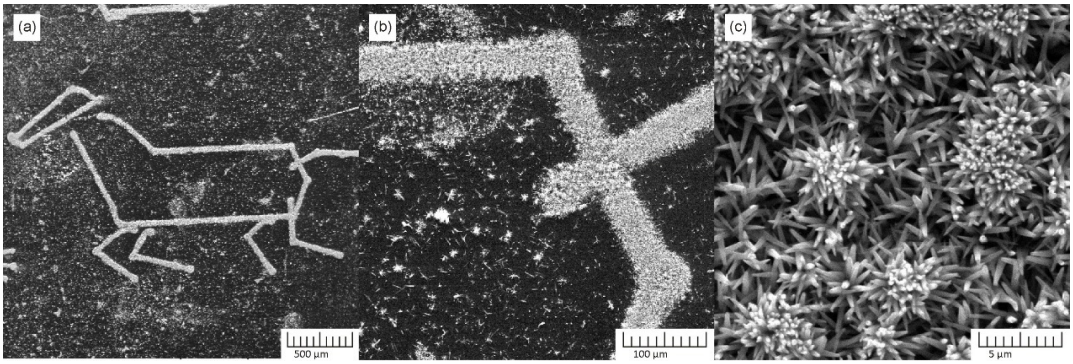

Fig. 6. ZnO nanostructures (at different magnifications) obtained on selectively laser-assisted seeds with the subsequent hydrothermal growth process in a working solution with an increased pH value.

As shown in Fig. 6a-c, in cases where nanostructures grow at increased pH, ultrasonic rinsing does not help to get rid of unwanted nanostructures. In this case, the contamination in the non-irradiated areas is much higher compared to the previous case, where growth took place in an equimolar working solution. Most likely, this is related to the stimulation and acceleration of the growth process of nanostructures. Under the influence of increased pH, the chemical reaction proceeds faster, and the required amount of OH ions is generated in a much shorter time. As the reaction speed increases, so does the speed of the nucleation process. A large number of ε-$Zn(OH)_2$ particles is massively generated in the volume of the solution. These particles form spherical aggregates with the aim of minimising the internal energy. As the number of surface nucleation bonds is small, a greater part of these aggregates fall into the sediment and form seeds which precipitate from solution and are fixed in arbitrary places, regardless of the presence of the seed layer. Comparing Fig. 6 and Fig. 5, it can be seen that in the case of an equimolar solution, the off-line space is much cleaner from contamination than a non-equimolar solution because the growth of nanostructures with a higher probability occurs only in energetically more favourable places (in this case on ZnO seeds).

Also, the change of other growth param-

eters (temperature, time) did not cause any significant external changes.

To completely get rid of the nanostructures formed outside the set line, a protective screen must be used during the growth process.

Within the framework of this experiment, we studied the effect of laser radiation power on the form of nuclei obtained from zinc acetate and, as a consequence, on the form of nanostructures obtained as a result of subsequent growth.

The experiment was repeated several times, changing the laser power in the range of 50-160 mW. After the end of the growth process, it could be concluded that the laser power increase leads to an increase in the width of the obtained line. The process is related to the heat transfer in metal, and with increasing the laser power, a larger area of zinc acetate is exposed to the temperature. No changes in the morphology and dimensions of the nanostructures were detected.

If we evaluate the results as a whole, the obtained ZnO nanostructures based on laser-obtained seeds do not differ in terms of morphology or size from the nanostructures obtained on zinc acetate seeds annealed in the furnace. It can be concluded that the parameters of the ZnO seeds are determined by the individual properties of the zinc acetate; the heat source is not important. The only necessary condition is exceeding the calcination temperature threshold (≈100-150 ºC); a further increase in temperature does not determine a change in the parameters of the seeds (obtainable nanostructures).

However, the use of a laser for the production of nuclei makes it possible to create unique and often very complex nanostructured patterns with elements several micrometres in size and clear lines with well-drawn boundaries, which is technically impossible to achieve when using the method of applying zinc acetate by dipping or stamping followed by thermal annealing.

3.3. Electrochemical Deposition

If it is necessary to coat metal electrodes with nanostructures, it is sometimes advisable to use the method of electrochemical deposition, which makes it possible to obtain a selective coating without the use of a seed layer.

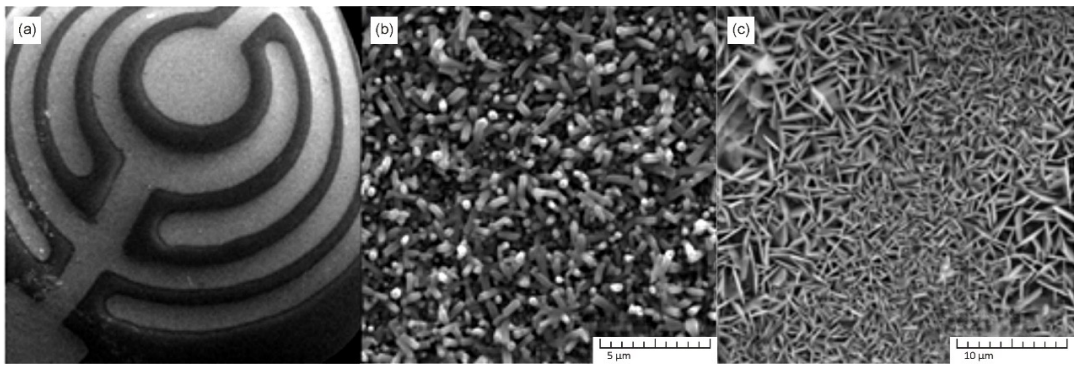

Fig. 7. ZnO nanostructures obtained by electrochemical deposition method. SEM overview of overgrown electrode (a), nanoneedles (b), nanoplates (c).

As shown in Fig. 7a, the growth of nanostructures is observed only on the electrodes: the interelectrode space is completely free of undesired nanostructures. The coating of both ZnO nanoneedles (Fig. 7b) and nanoplates (Fig. 7c) is dense and homoge-

neous. The crystallites of both morphologies are very similar in shape and size to those obtained by hydrothermal synthesis.

It should be noted that, unlike a classical hydrothermal synthesis, the electrochemical deposition method requires a definition of precise experimental conditions, such as potentials, reactants, concentrations, pH, deposition times, etc. Even the smallest deviation from the optimum growth process affects the quality of the sample surface (an amorphous layer can be formed instead of nanostructures). Very strict requirements are imposed on the electric conductivity of the electrode material, and the optimal growth parameters must be determined for each kind of substrate (unlike hydrothermal synthesis, where the result is predictable for all surface types and does not depend on the substrate material).

Another factor to consider is the electrochemical corrosion of the forced contacts. Although the contact area of the electrodes is not in direct contact with the working solution, they are exposed to water vapour for a long time because growth takes place at a relatively high temperature (80 ºC). However, despite all the complicating factors, the method proved to be very effective. In cases where it is necessary to cover small electrodes with nanostructures and keep the outside electrode space clean, this method is very useful, accurate, and fast. This method becomes especially relevant when, for a number of reasons, the deposition of nuclei is impossible or it is necessary to obtain oxides of different metals on one electrode.

4. CONCLUSIONS

All of the methods discussed in the article provide for a good selective area growth of nanostructures and allow the formation of intricately shaped nanostructured patterns on different types of surfaces.

Regardless of the method of obtaining the ZnO seeds, using an extra cover screen helps restrict the surface from the effects of convection flows of the solution and reduces the likelihood of nanostructures outside the patterned area.

For the selective patterning of the zinc oxide seed layer by using the stamping transfer process, it is recommended to apply zinc acetate on a preheated substrate to reduce the thermocapillary effect and homogenise the coating.

The morphology of the obtained ZnO nanostructures does not depend on the methods of obtaining seeds: decomposition of zinc acetate during annealing in a furnace or selective laser decomposition. The only condition required is that the calcination temperature threshold is exceeded (≈100–150 °C). A further increase in temperature does not determine the change of seed parameters (obtainable nanostructures). Thus, the heat source is not significant.

Of all the above-mentioned methods, the electrochemical synthesis method has the highest requirements for observing synthesis parameters and surface quality. It is sensitive to current and temperature changes during the synthesis process and can only be used for coating conductive surfaces. However, this method is optimal in cases where electrodes of various shapes have to be covered with nanostructures. It is fast because the growth takes place immediately over the entire area, and it is precise because it allows covering elements in the range of a few microns.

ACKNOWLEDGEMENTS

The research has been supported by ERDF project No. 1.1.1.2/VIAA/4/20/743 "Development of Nanomaterial-based Electrochemical Sensor for Detection of Hydrogen Peroxide".

REFERENCES

1. Santos, M. S., Marques Lameirinhas, R. A., N. Torres, J. P., P. Fernandes, J. F., & Correia V. Bernardo, C. P. (2023). Nanostructures for Solar Energy Harvesting. *Micromachines*, *14*, 364. doi:10.3390/mi14020364.
2. Sidorenko, A. S. (2020). Functional Nanostructures for Electronics, Spintronics and Sensors. *Beilstein J. Nanotechnol., 11*, 1704–1706. doi: 10.3762/bjnano.11.152.
3. Mitchell, M. J., Billingsley, M. M., Haley, R. M., Wechsler, M. E., Peppas, N. A., & Langer, R. (2021). Engineering Precision Nanoparticles for Drug Delivery. *Nat. Rev. Drug Discov., 20*, 101–124. doi: 10.1038/s41573-020-0090-8.
4. Arredondo-Ochoa, T., & Silva-Martínez, G. A. (2022). Microemulsion Based Nanostructures for Drug Delivery. *Front. Nanotechnol., 3,* 753947. doi: 10.3389/fnano.2021.753947.
5. Gautam, Y. K., Sharma, K., Tyagi, S., Ambedkar, A. K., Chaudhary, M., & Pal Singh, B. (2021). Nanostructured Metal Oxide Semiconductor-Based Sensors for Greenhouse Gas Detection: Progress and Challenges. *R. Soc. Open Sci., 8*, 201324. doi: 10.1098/rsos.201324.
6. Gorup, L. F., Sequinel, T., Akucevicius, G. W., Pinto, A. H., Biasotto, G., Ramesar, N., de Arruda, E., G., R., … & Camargo, E. R. (2021). Nanostructured Gas Sensors in Smart Manufacturing. *Nanosensors for Smart Manufacturing, Elsevier,* 445–485. doi.org/10.1016/B978-0-12-823358-0.00022-8.
7. Chowdhury, N. K., & Bhowmik, B. (2021). Micro/Nanostructured Gas Sensors: The Physics behind the Nanostructure Growth, Sensing and Selectivity Mechanisms. *Nanoscale Adv., 3,* 73–93. doi: 10.1039/d0na00552e.
8. Karabulut, G., Beköz Üllen, N., & Karakuş, S. (2022). Nanostructures in Biosensors: Development and Applications. *Biomedical Engineering. IntechOpen.* doi: 10.5772/intechopen.108508.
9. Varnakavi Naresh, V., & Lee, N. (2021). A Review on Biosensors and Recent Development of Nanostructured Materials-Enabled Biosensors. *Sensors (Basel), 21* (4), 1109. doi: 10.3390/s21041109.
10. Bertel, L., Miranda, D. A., & García-Martín, J. M. (2021). Nanostructured Titanium Dioxide Surfaces for Electrochemical Biosensing. *Sensors, 21*, 6167. doi: 10.3390/s21186167.
11. Nagal, V., Masrat, S., Khan, M., Alam, S., Ahmad, A.; Alshammari, M. B., ... & Ahmad, R. (2023). Highly Sensitive Electrochemical Non-Enzymatic Uric Acid Sensor Based on Cobalt Oxide Puffy Balls-like Nanostructure. *Biosensors, 13*, 375. doi: 10.3390/bios13030375.
12. Abdel-Karim, R., Reda, Y., & Abdel-Fattah, A. (2020). Review—Nanostructured Materials-Based Nanosensors. *J. Electrochem. Soc., 167*, 037554. doi: 10.1149/1945-7111/ab67aa.
13. Macagnano, A., & Avossa, J. (2020). Chapter 11 – Nanostructured composite materials for advanced chemical sensors. In *Advances in Nanostructured Materials and Nanopatterning Technologies: Applications for Healthcare, Environment and Energy*, *Elsevier,* (pp. 297–332). doi: 10.1016/b978-0-12-816865-3.00011-1.

14. Gerbreders, V., Krasovska, M., Mihailova, I., Ogurcovs, A., Sledevskis, E., Gerbreders, A., … & Plaksenkova, I. (2021). Nanostructure-Based Electrochemical Sensor: Glyphosate Detection and the Analysis of Genetic Changes in Rye DNA. *Surfaces and Interfaces, 26*, 101332. doi: 10.1016/j.surfin.2021.101332.
15. Nagal, V., Tuba, T., Kumar, V., Alam, S., Ahmad, A., Alshammari, M. B., … & Ahmad, R. (2022). A Non-enzymatic Electrochemical Sensor Composed of Nano-berry Shaped Cobalt Oxide Nanostructures on a Glassy Carbon Electrode for Uric Acid Detection. *New J. Chem., 46*, 12333–12341. doi: 10.1039/D2NJ01961B.
16. Fall, B., Sall, D. D., Hémadi, M., Diaw, A. K. D., Fall, M., Randriamahazaka, H., & Thomas, S. (2023). Highly Efficient Non-enzymatic Electrochemical Glucose Sensor Based on Carbon Nanotubes Functionalized by Molybdenum Disulfide and Decorated with Nickel Nanoparticles (GCE/CNT/MoS_2/NiNPs). *Sens. Actuat. Rep., 5*, 100136. doi: 10.1016/j.snr.2022.100136.
17. Singer, N., Pillai, R. G., Johnson, A. I. D., Harris, K. D., & Jemere, A. B. (2020). Nanostructured Nickel Oxide Electrodes for Non-enzymatic Electrochemical Glucose Sensing. *Microchimica Acta, 187* (4), 187–196. doi: 10.1007/s00604-020-4171-5.
18. Echarri-Giacchi, M., & Martín-Martínez J. M. (2022). Efficient Physical Mixing of Small Amounts of Nanosilica Dispersion and Waterborne Polyurethane by Using Mild Stirring Conditions. *Polymers, 14*(23), 5136. doi: 10.3390/polym14235136.
19. Liao, M.-J., & Duan, L.-Q. (2020). Dependencies of Surface Condensation on the Wettability and Nanostructure Size Differences. *Nanomaterials (Basel)., 10* (9), 1831. doi: 10.3390/nano10091831.
20. Shen, J.-F., Wu, C.-M., Mo, D.-M., & Lio, Y.-R. (2023). Molecular Investigation on the Formation and Transition of Condensation Mode on the Surface with Nanostructure. *J. Mol. Liq., 369*, 120848. doi: 10.1016/j.molliq.2022.120848.
21. Jinming Liu, J., He, S.- H., & Wang, J.- P. (2020). High-Yield Gas-Phase Condensation Synthesis of Nanoparticles to Enable a Wide Array of Applications. *ACS Appl. Nano Mater., 3* (8), 7942–7949. doi:10.1021/acsanm.0c01400.
22. Parauha, Y. R., Sahu, V., & Dhoble, S. J. (2021). Prospective of Combustion Method for Preparation of Nanomaterials: A Challenge. *Mater. Sci. Eng.: B, 267*, 115054. doi: 10.1016/j.mseb.2021.115054.
23. Wahyudiono, Kondo, H., Yamada, M., Takada, N., Machmudah, S., Kanda, H., & Goto, M. (2020). DC-Plasma over Aqueous Solution for the Synthesis of Titanium Dioxide Nanoparticles under Pressurized Argon. *ACS Omega, 5* (10), 5443–5451. doi: 10.1021/acsomega.0c00059.
24. Li, Z., Coll, M., Mundet, B., Chamorro, N., Vallès, F., Palau, A., Gazquez, J., ... & Obradors, X. (2019). Control of Nanostructure and Pinning Properties in Solution Deposited $YBa_2Cu_3O_{7-x}$ Nanocomposites with Preformed Perovskite Nanoparticles. *Sci. Rep., 9* (1)*,* 5828. doi: 10.1038/s41598-019-42291-x.
25. Gan, Y. X., Jayatissa, A. H., Yu, Z., Chen, X., & Li, M. (2020). Hydrothermal Synthesis of Nanomaterials. *J. Nanomater., 2020,* 8917013. doi: 10.1155/2020/8917013.
26. Bokov, D., Jalil, A. T., Chupradit, S., Suksatan, W., Ansari, M. J., Shewael, I. H., ... & Kianfar, E. (2021). Nanomaterial by Sol-Gel Method: Synthesis and Application. *Adv. Mater. Sci. Eng.*, *2021*, 5102014. doi: 10.1155/2021/5102014.
27. Navas, D., Fuentes, S., Castro-Alvarez, A., & Chavez-Angel, E. (2021). Review on Sol-Gel Synthesis of Perovskite and Oxide Nanomaterials. *Gels, 7*, 275. doi: 10.3390/gels7040275.
28. Yarbrough, R., Davis, K., Dawood, S., & Rathnayake, H. (2020). A Sol–Gel Synthesis to Prepare Size and Shape-Controlled Mesoporous Nanostructures of Binary (II–VI) Metal Oxides. *RSC Adv., 10*, 14134–14146. doi: 10.1039/D0RA01778G.
29. Domonkos, M., & Kromka, A. (2022). Nanosphere Lithography-Based Fabrication of Spherical Nanostructures and Verification of Their Hexagonal Symmetries by Image Analysis. *Symmetry, 14,* 2642. doi: 10.3390/sym14122642.

30. Jang, H.-I., Yoon, H.-S., Lee, T.-I., Lee, S., Kim, T.-S., Shim, J., & Park, J. H. (2020). Creation of Curved Nanostructures Using Soft-Materials-Derived Lithography. *Nanomaterials***,** *10 (12)*, 2414. doi: 10.3390/nano10122414.
31. Qu, J., Yang, W., Wu, T., Ren, W., Huang, J., Yu, H., … & CairneyJ. M. (2022). Atom Probe Specimen Preparation Methods for Nanoparticles. *Ultramicroscopy, 233*, 113420. doi: 10.1016/j.ultramic.2021.113420.
32. Shahzad, S., Javed, S., & Usman, M. (2021). A Review on Synthesis and Optoelectronic Applications of Nanostructured ZnO. *Front. Mater., 8*, 613825. doi: 10.3389/fmats.2021.613825.
33. Djurišić, A. B., Ng, A. M. C., & Chen, X. (2010). ZnO Nanostructures for Optoelectronics: Material Properties and Device Application. *Progress in Quantum Electronics, 34* (4), 191–259. doi:10.1016/j.pquantelec.2010.04.001.
34. Jiang, J., Pi, J., & Cai, J. (2018). The Advancing of Zinc Oxide Nanoparticles for Biomedical Applications. *Bioinorg. Chem. Appl., 2018,* 1062562. doi: 10.1155/2018/1062562.
35. Barman, A. (2015). Review on biocompatibility of ZnO nano particles. In Gupta, S., Bag, S., Ganguly, K., Sarkar, I., Biswas, P. (eds.) *Advancements of Medical Electronics. Lecture Notes in Bioengineering*. (pp. 343–352). Springer, New Delhi. doi: 10.1007/978-81-322-2256-9_32.
36. Oleshko, O., Husak, Y., Korniienko, V., Pshenychnyi, R., Varava, Y., Kalinkevich, O., ... & Pogorielov, M. (2020). Biocompatibility and Antibacterial Properties of ZnO-Incorporated Anodic Oxide Coatings on TiZrNb Alloy. *Nanomaterials (Basel), 10* (12), 2401. doi:10.3390/nano10122401.
37. Krishna, M. S., Sing, S., Batool, M., Fahmy, H. M., Seku, K., Shalan, A. E., … & Zafar, M. N. (2023). A Review on 2D-ZnO Nanostructure Based Biosensors: From Materials to Devices. *Mater. Adv., 4*, 320–354. doi: 10.1039/d2ma00878e.
38. Yang, G., & Park, S.-J. (2019). Conventional and Microwave Hydrothermal Synthesis and Application of Functional Materials: A Review. *Materials (Basel), 12* (7), 1177. doi:10.3390/ma12071177.
39. Adeleye, A. T., John, K. I., Adeleye, P. G., Akande, A. A., & Banjoko, O. O. (2021). One-dimensional Titanate Nanotube Materials: Heterogeneous Solid Catalysts for Sustainable Synthesis of Biofuel Precursors/Value-Added Chemicals – A Review. *J. Mater. Sci., 56* (5), 18391–18416. doi: 10.1007/s10853-021-06473-1.
40. Gerbreders, V., Krasovska, M., Sledevskis, E., Gerbreders, A., Mihailova, I., & Ogurcovs, A. (2020). Hydrothermal Synthesis of ZnO Nanostructures with Controllable Morphology Change. *CrystEngComm, 22*, 1346–1358. doi:10.1039/C9CE01556F.
41. Xu, S., Lao, C., Weintraub, B., & Wang, Z. L. (2008). Density-Controlled Growth of Aligned ZnO Nanowire Arrays by Seedless Chemical Approach on Smooth Surfaces. *J. Mater. Res., 23* (08)*,* 2072–2077. doi:10.1557/jmr.2008.0274.
42. Krasovska, M., Gerbreders, V., Paskevics, V., Ogurcovs, A., & Mihailova, I. (2015). Obtaining a Well-Aligned ZnO Nanotube Array Using the Hydrothermal Growth Method. *Latvian Journal of Physics and Technical Sciences, 52* (5)*,* 28–40. doi:10.1515/lpts-2015-0026.
43. Gerbreders, V., Krasovska, M., Mihailova, I., Sledevskis, E., Ogurcovs, A., Tamanis, E., … & Mizers, V. (2022). Morphology Influence on Wettability and Wetting Dynamics of ZnO Nanostructure Arrays. *Latvian Journal of Physics and Technical Sciences*, *59* (1), 30–43. doi: 10.2478/lpts-2022-0004.
44. Gerbreders, V., Krasovska, M., Mihailova, I., Ogurcovs, A., Sledevskis, E., Gerbreders, A., …& Plaksenkova, I. (2019). ZnO Nanostructure-Based Electrochemical Biosensor for Trichinella DNA Detection. *Sensing and Bio-Sensing Research, 23,* 100276. doi: 10.1016/j.sbsr.2019.100276.

45. Schürch, P., Osenberg, D., Testa, P., Bürki, G., Schwiedrzik, J., Michler, J., & Koelmans, W. W. (2023). Direct 3D Microprinting of Highly Conductive Gold Structures via Localized Electrodeposition. *Materials & Design*, *227*, 111780. doi: 10.1016/j.matdes.2023.111780.
46. Muldoon, K., Song, Y., Ahmad, Z., Chen, X., & Chang, M.-W. (2022). High Precision 3D Printing for Micro to Nano Scale Biomedical and Electronic Devices. *Micromachines (Basel), 13* (4), 642. doi: 10.3390/mi13040642.
47. Tsangarides, C. T., Ma, H., & Nathan, A. (2016). ZnO Nanowire Array Growth on Precisely Controlled Patterns of Inkjet-Printed Zinc Acetate at Low-Temperatures. *Nanoscale, 8*, 11760–11765. doi: 10.1039/c6nr02962k.
48. Wang, X., Sun, F., Huang, Y., Duan, Y., & Yin, Z. (2015). Patterned ZnO Nanorod Array/Gas Sensor by Mechanoelectrospinning-Assisted Selective Growth. *ChemComm, 51* (15), 3117–3120. doi:10.1039/c4cc08876j.
49. Lee, D., Tang, Y.-L., & Liu, S.-J. (2021). Fast Fabrication of Nanostructured Films Using Nanocolloid Lithography and UV Soft Mold Roller Embossing: Effects of Processing Parameters. *Polymers*, *13* (3), 405. doi:10.3390/polym13030405.
50. Lee, Y. H., Ke, K. C., Chang, N.W. & Yang, S. Y. (2018). Development of an UV Rolling System for Fabrication of Micro/Nano Structure on Polymeric Films Using a Gas-Roller-Sustained Seamless PDMS Mold. *Microsyst. Technol., 24* (7), 2941–2948. doi:10.1007/s00542-017-3683-3.
51. Fung, C. M., Lloyd, J. S., Samavat, S., Deganello, D., & Tenga, K. S. (2017). Facile Fabrication of Electrochemical ZnO Nanowire Glucose Biosensorusing Roll to Roll Printing Technique. *Sens. Actuat. B: Chem., 247*, 807–813. doi: 10.1016/j.snb.2017.03.105.
52. Kim, S., Sojoudi, H., Zhao, H., Mariappan, D., McKinley, G. H., Gleason, K. K., & Hart, A. J. (2016). Ultrathin High-Resolution Flexographic Printing Using Nanoporous Stamps. *Sci Adv., 2* (12), e1601660. doi: 10.1126/sciadv.1601660.
53. Kim, M., Oh, D., Kim, J., Jeong, M., Kim, H., Jung, C., ... & Ok, J. (2022). Facile Fabrication of Stretchable Photonic Ag Nanostructures by Soft-Contact Patterning of Ionic Ag Solution Coatings. *Nanophotonics*, *11* (11), 2693–2700. doi: 10.1515/nanoph-2021-0812.
54. Donie, Y. J., Yuan, Y., Allegro, I., Schackmar, F., Hossain, I. M., Huber, R., ... & Lemmer, U. (2022). A Self-Assembly Method for Tunable and Scalable Nano-Stamps: A Versatile Approach for Imprinting Nanostructures. *Adv. Mater. Technol., 7* (6), 2101008. doi: 10.1002/admt.202101008.
55. Taus, P., Prinz, A., Wanzenboeck, H. D., Schuller, P., Tsenov, A., Schinnerl, M., … & Muehlberger, M. (2021). Mastering of NIL Stamps with Undercut T-Shaped Features from Single Layer to Multilayer Stamps. *Nanomaterials*, *11*, 956. doi: 10.3390/nano11040956.
56. Liu, Z., Liu, N., & Schroers, J. (2022). Nanofabrication through Molding. *Progress Mater. Sci., 125,* 100891. doi: 10.1016/j.pmatsci.2021.100891.
57. Kang, H. W., Yeo, J., Hwang, J. O., Hong, S., Lee, P., Han, S. Y., … & Sung,H. J. (2011). Simple ZnO Nanowires Patterned Growth by Microcontact Printing for High Performance Field Emission Device. *J. Phys. Chem. C, 115* (23), 11435–11441. doi:10.1021/jp2019044.
58. Chakraborty, A., Orsini, A., Kar, J. P., Gatta, F., Khan, U., & Falconi, C. (2022). Ultra-efficient Thermo-convective Solution-Growth of Vertically Aligned ZnO Nanowires. *Nano Energy, 97*, 107167. doi: 10.1016/j.nanoen.2022.107167.
59. Simon Xia, S., Mostafavi, M., Alghazali, T., Sajad sadi, Guerrero, J. W. G., Suksatan, W., … & Khan, A. (2022). Numerical Investigation of Nanofluid Mixed Convection in a T-shaped Cavity by Considering a Thermal Barrier. *Alexandria Eng. J., 61* (9), 7393–7415. doi: 10.1016/j.aej.2022.01.009.
60. Ko, S. H., Lee, D., Hotz, N., Yeo, J., Hong, S., Nam, K. H., & Grigoropoulos, C. P. (2011). Digital Selective Growth of ZnO Nanowire Arrays from Inkjet-Printed Nanoparticle Seeds on a Flexible Substrate. *Langmuir, 28* (10), 4787–4792. doi:10.1021/la203781x.

61. Šimáková, P., Kočišová, E., & Procházka, M. (2021). “Coffee Ring” Effect of Ag Colloidal Nanoparticles Dried on Glass: Impact to Surface-Enhanced Raman Scattering (SERS). *J. Nanomater., 2021*, 4009352. doi: 10.1155/2021/4009352.
62. Sliz, R., Czajkowski, J., & Fabritius, T. (2020). Taming the Coffee Ring Effect – Enhanced Thermal Control as Method for Thin-Films Nanopatterning. *Langmuir, 36* (32), 9562–9570. doi:10.1021/acs.langmuir.0c01560.
63. Kwon, J., Hong, S., Lee, H., Yeo, J., Lee, S. S., & Ko, S. H. (2013). Direct Selective Growth of ZnO Nanowire Arrays from Inkjet-Printed Zinc Acetate Precursor on a Heated Substrate. *Nanoscale Res. Lett., 8* (1), 489. doi.: 10.1186/1556-276X-8-489.
64. Hong, S., Yeo, J., Manorotkul, W., Kang, H. W., Lee, J., Han, S., … & Ko, S. H. (2013). Digital Selective Growth of a ZnO Nanowire Array by Large Scale Laser Decomposition of Zinc Acetate. *Nanoscale, 5* (9)*,* 3698–3703. doi: 10.1039/c3nr34346d.
65. Guo, X. D., Pi, H. Y., Zhao, Q. Z., & Li, R. X. (2012). Controllable Growth of Flowerlike ZnO Nanostructures by Combining Laser Direct Writing and Hydrothermal Synthesis. *Mater. Lett., 66*, 377–381. doi: 10.1016/j.matlet.2011.09.008.
66. Hong, S., Yeo, J., Manorotkul, W., Kim, G., Kwon, J., An, K., & Ko, S. H. (2013). Low-Temperature Rapid Fabrication of ZnO Nanowire UV Sensor Array by Laser-Induced Local Hydrothermal Growth. J. *Nanomater., 2013*, 246328. doi:10.1155/2013/246328.
67. In, J. B., Kwon, H.-J., Lee, D., Ko, S. H., & Grigoropoulos, C. P. (2013). In Situ Monitoring of Laser-Assisted Hydrothermal Growth of ZnO Nanowires: Thermally Deactivating Growth Kinetics. *Small, 10* (4), 741–749. doi:10.1002/smll.201301599.
68. Liu, W. L., Chang, Y. C., Hsieh, S. H., & Chen,W. J. (2013). Effects of Anions in Electrodeposition Baths on Morphologies of Zinc Oxide Thin Films. *Int. J. Electrochem. Sci., 8* (1), 983–990. http://www.electrochemsci.org/papers/vol8/80100983.pdf
69. Jiangfeng, G., Zhaoming, D., Qingping, D., Yuan,X., & Weihua, Z. (2010). Controlled Synthesis of ZnO Nanostructures by Electrodeposition Method. *J. Nanomater., 2010*, 740628. doi: 10.1155/2010/740628.
70. Lin, Y., Yang, J., & Zhou, X. (2011). Controlled Synthesis of Oriented ZnO Nanorod Arrays by Seed-Layer-Free Electrochemical Deposition. *Appl. Surface Sci., 258* (4), 1491–1494. doi: 10.1016/j.apsusc.2011.09.113.
71. Sun, S., Jiao, S., Zhang, K., Wang, D., Gao, S., Li, H., … & Zhao, L. (2012). Nucleation Effect and Growth Mechanism of ZnO Nanostructures Electrodeposition from Aqueous Zinc Nitrate Baths. *J. Crystal Growth, 359*, 15–19. doi: 10.1016/j.jcrysgro.2012.08.016.
72. Xu, L., Guo, Y., Liao, Q., Zhang, J., & Xu, D. (2005). Morphological Control of ZnO Nanostructures by Electrodeposition. *J. Phys. Chem. B, 109* (28), 13519–13522. doi: 10.1021/jp051007b.
73. Skompska, M., & Zarębska, K. (2014). Electrodeposition of ZnO Nanorod Arrays on Transparent Conducting Substrates – A Review. *Electrochim. Acta, 127,* 467–488. doi: 10.1016/j.electacta.2014.02.049.